On-surface polymerisation and self-assembly of DPP-based molecular wires

Michael Clarke[1], Abigail Bellamy-Carter[2], Ferdinando Malagreca[3], Jack Hart[1], Stephen P. Argent[3], James O'Shea[1], David B. Amabilino[4], Alex Saywell[1*]

[1]School of Physics & Astronomy, University of Nottingham, Nottingham NG7 2RD, United Kingdom

[2]School of Liberal Arts and Natural Sciences, University of Birmingham, Edgbaston, Birmingham B15 2TT, United Kingdom

[3]School of Chemistry, University of Nottingham, Nottingham NG7 2RD, United Kingdom

[4]Institut de Ciència de Materials de Barcelona (ICMAB-CSIC), Campus Universitari de Bellaterra, 08193 Cerdanyola del Vallès, Spain

[*]alex.saywell@nottingham.ac.uk

1-Materials and methods

All commercially available reagents and solvents were used as received. Chromatography purifications were performed using Sigma-Aldrich Silica Gel (pore size 60Å, particle size 40- 63 µm) and thin-layer chromatography (TLC) was carried out on E. Merck silica gel plates, irradiated using UV light (365 nm). NMR spectra were acquired on a Bruker AV400, Bruker AV(III)500, Jeol EX270 or Bruker DPX300 spectrometers and NMR spectra were recorded at room temperature, unless otherwise stated. All chemical shifts are reported in δ parts per million (ppm), using the solvent residual signal as an internal standard and the coupling constant values (*J*) are reported in hertz (Hz). The following abbreviations are used for signal multiplicities: s, singlet; d, doublet; t, triplet; m, multiplet; and b, broad. Infra-red spectra were recorded on a Bruker Tensor 27 instrument equipped with a Pike GladiATR attachment with a diamond crystal.

For **Br_2Hex_2DPP** single crystal was selected and mounted using Fomblin® (YR-1800 perfluoropolyether oil) on a polymer-tipped MiTeGen MicroMountTM and cooled rapidly to 120 K in a stream of cold N_2 using an Oxford Cryosystems open flow cryostat[1]. Single crystal X-ray diffraction data were collected on an Oxford Diffraction SuperNova diffractometer (Atlas CCD area detector, mirror-monochromated Cu-Kα radiation source; λ = 1.54184 Å). Cell parameters were refined from the observed positions of all strong reflections and absorption corrections were applied using a Gaussian numerical method with beam profile correction (CrysAlisPro)[2]. The structures were solved within Olex2[3] by dual space iterative methods (SHELXT)[4] least squares refinement of the structure was carried using (SHELXL)[5]. Structures were checked with checkCIF[6]. CCDC-2208888. These data can be obtained free of charge from The Cambridge Crystallographic Data Centre via www.ccdc.cam.ac.uk/data_request/cif.

2-Synthesis

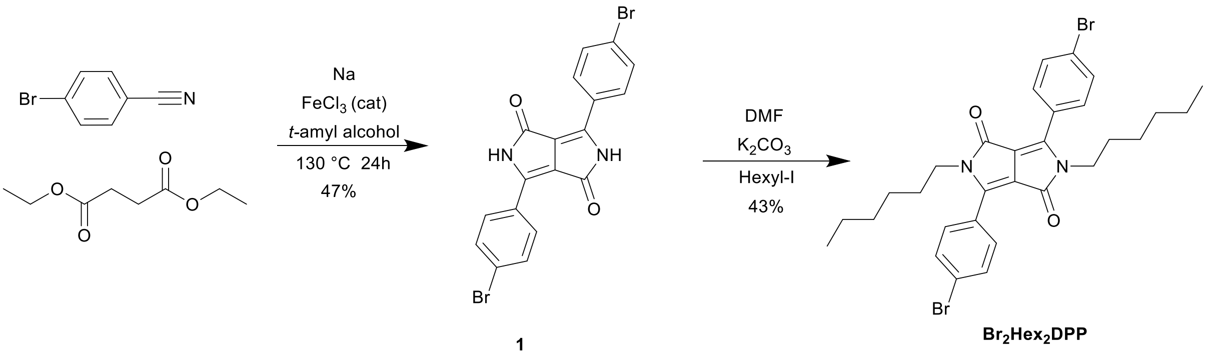

Scheme S1. Synthesis of **Br_2Hex_2DPP**

Synthesis of 3,6-bis(4-bromophenyl)pyrrolo[3,4-c]pyrrole-1,4(2H,5H)-dione. (**1**)

Sodium (1.26 g, 54.94 mmol) and $FeCl_3$ (cat) was added to dry *t*-amyl alcohol (27.5 ml), and the mixture was stirred at 90 °C. After the sodium was completely dissolved, 4-bromobenzonitrile (5.00 g, 27.47 mmol) was added at 50 °C. The temperature was raised to 90 °C, and diethyl succinate (5.0 ml, 3.0 mmol) in 11.5 ml of 2-methyl-2-butanol was added drop wise. The mixture was stirred at 90 °C for 24 hours. Acetic acid (11.5 ml) was added drop wise to the mixture and was stirred at 120 °C for 1 hour. The reaction mixture was allowed to cool down to room temperature and was filtered. The filtered dark red solid was washed with water and methanol several times and used for next reaction without further purification. Product 2.29 g, (47%) FT-ATR-IR : 3139 (N–H stretching), 1641 (C=O stretching), 1604 (N–H bending or Ar–C=C stretching), 1533, 1490, 1438, 1390, 819 cm^{-1}.

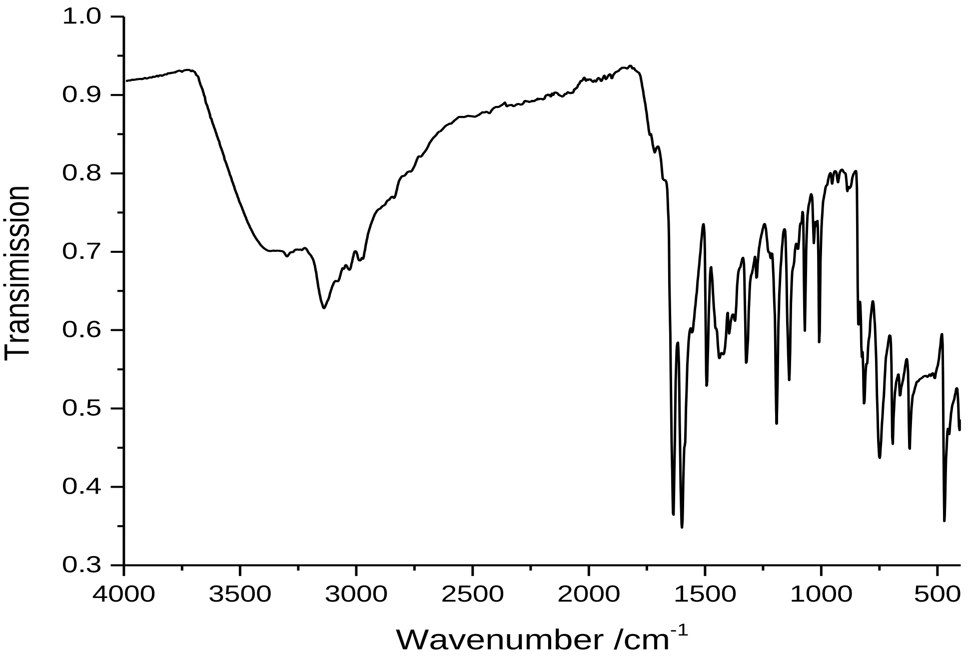

Figure S1. FT-IR of **1**

Synthesis of 2,5-bishexyl-3,6-bis(4-bromophenyl)-2,5-dihydropyrrolo[3,4-c]pyrrole-1,4-dione (**Br_2Hex_2DPP**)

3,6-Bis(4-bromophenyl)pyrrolo[3,4-c]pyrrole-1,4(2H,5H)-dione (1 g, 2.24 mmol), Cs_2CO_3 (2.19 g, 6.72 mmol) and 1-hexyl Iodine (1.73 g, 8.97 mmol) were combined in dry dimethylformamide (25 ml). The mixture was stirred at 40 °C for 24 hr. After cooling to room temperature, the mixture was poured into water and extracted with dichloromethane. The organic phase was dried over $MgSO_4$ and the solvent was evaporated *in vacuo* after filtration. The compound was precipitated from methanol and recrystallized in the same solvent to obtain an orange solid of **Br_2Hex_2DPP**. Product 0.65 g (43%). FT-ATR-IR : 2951 (CH stretch), 2924(CH stretch), 2854 (CH stretch), 1672(C=O), 1610, 1485(C=C stretch), 1456, 1400, 1384, 1348, 1163, 1087, 1087, 1006, 972, 896, 833, 733, 673, 621, 509, 460, 405 cm^{-1}; ^{1}H NMR ($CDCl_3$, 400 MHz, ppm): δ 7.58–7.56 (m, 4H), 7.53–7.51 (m, 4H), 3.68 (t, *J* = 7.6 Hz, 4H), 1.46–1.43 (m, 4H), 1.22–1.16 (m, 12H), 0.83–0.79 (m, 6H) ppm. ^{13}C NMR (75 MHz, $CDCl_3$) δ 162.4, 147.4, 132.3, 130.0, 126.9, 125.8, 109.1, 41,9, 31.9, 29.4, 26.3, 22.4.

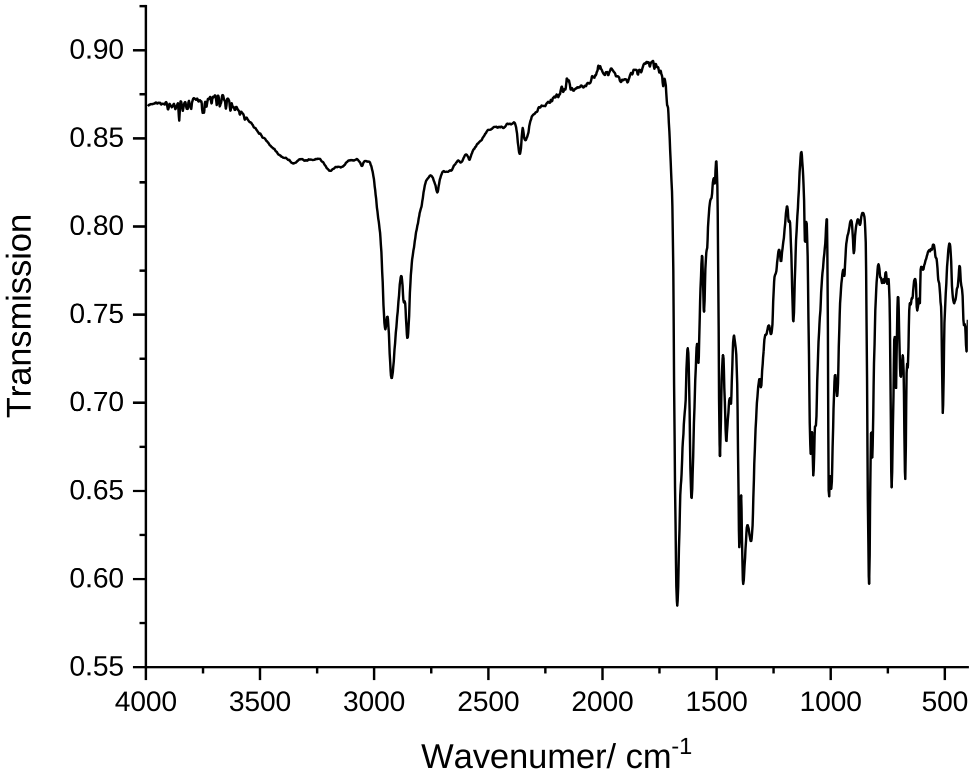

Figure S2. FT-IR of **Br_2Hex_2DPP**

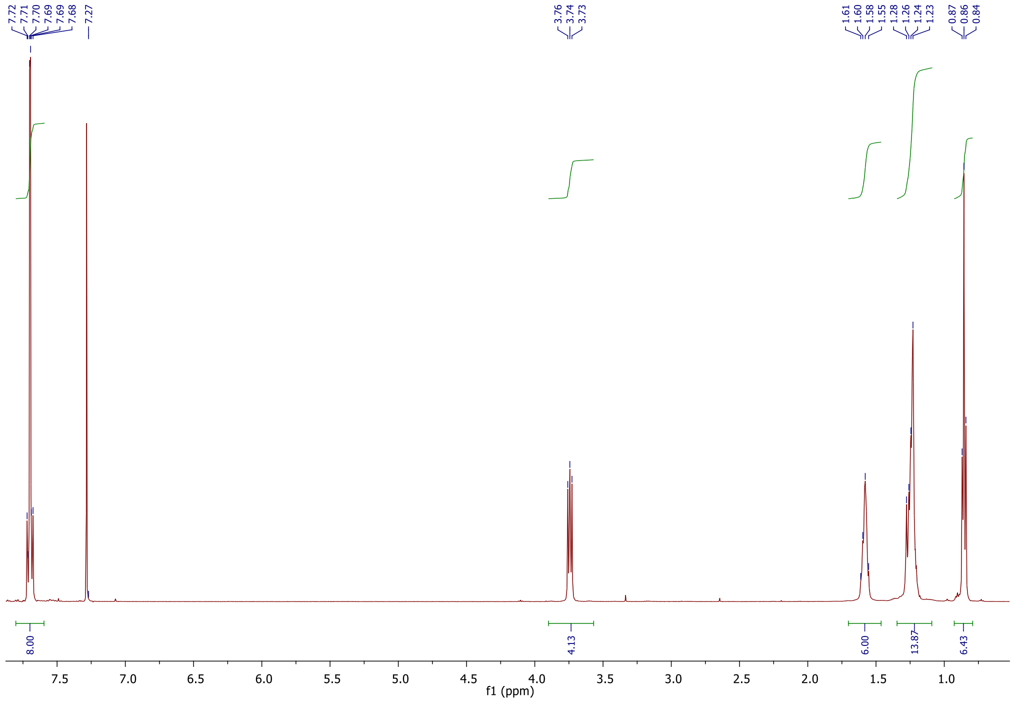

Figure S3. ^{1}H NMR of **Br_2Hex_2DPP** recorded in $CDCl_3$

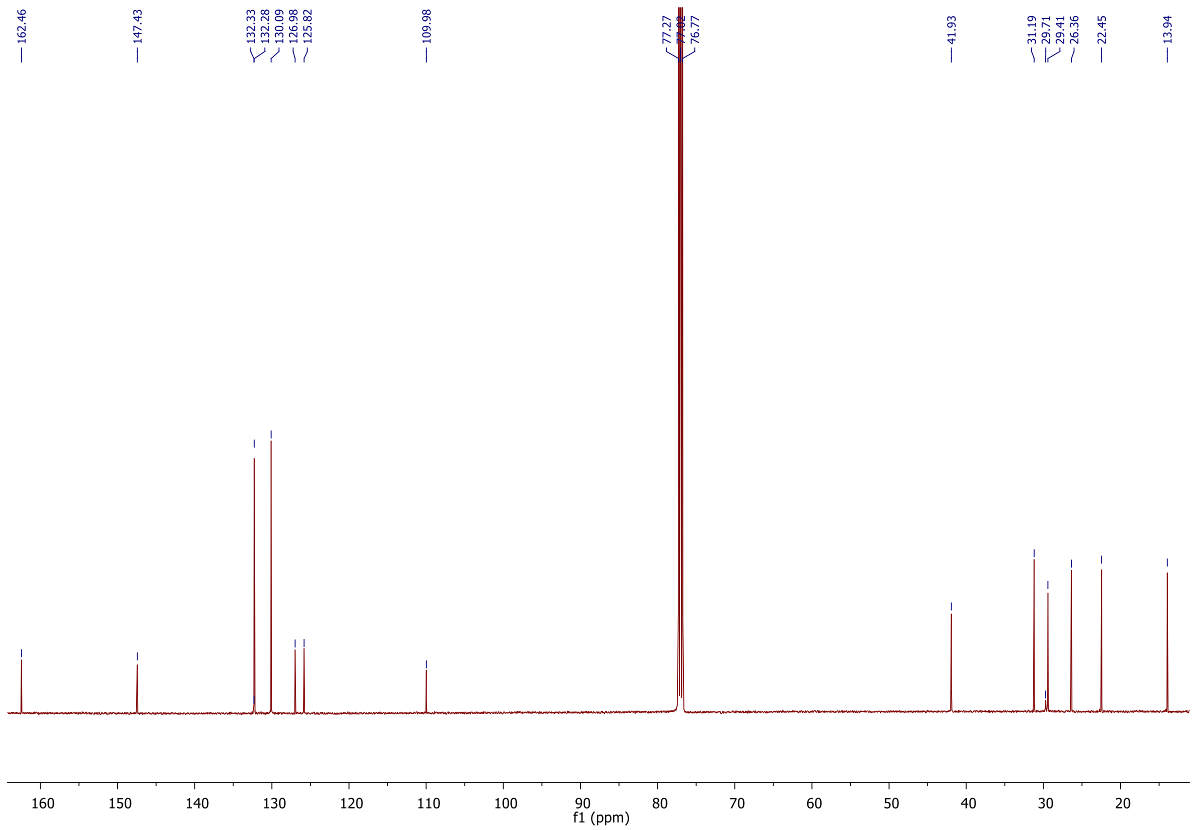

Figure S4. ^{13}C NMR of **Br$_2$Hex$_2$DPP** recorded in CDCl$_3$.

3- Crystallographic information

Table 1. Experimental details

	Br_2Hex_2DPP
Crystal data	
Chemical formula	$C_{30}H_{34}Br_2N_2O_2$
M_r	614.41
Crystal system, space group	Triclinic, *P*-1
Temperature (K)	120
a, *b*, *c* (Å)	14.6708 (5), 15.2829 (6), 15.5753 (4)
α, β, γ (°)	106.052 (3), 103.399 (3), 115.453 (4)
V (Å^3)	2771.97 (19)
Z	4
Radiation type	Cu *K*α
μ (mm^{-1})	3.94
Crystal size (mm)	0.21 × 0.17 × 0.11
CCDC	2208888

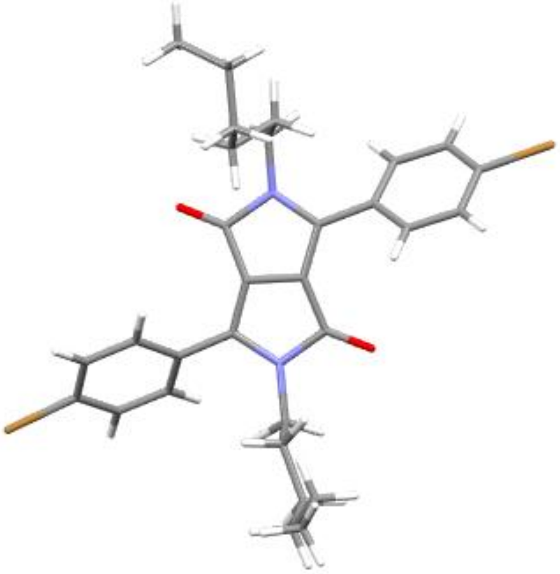

Figure S5. Crystal structure of **Br_2Hex_2DPP** showing a single molecule.

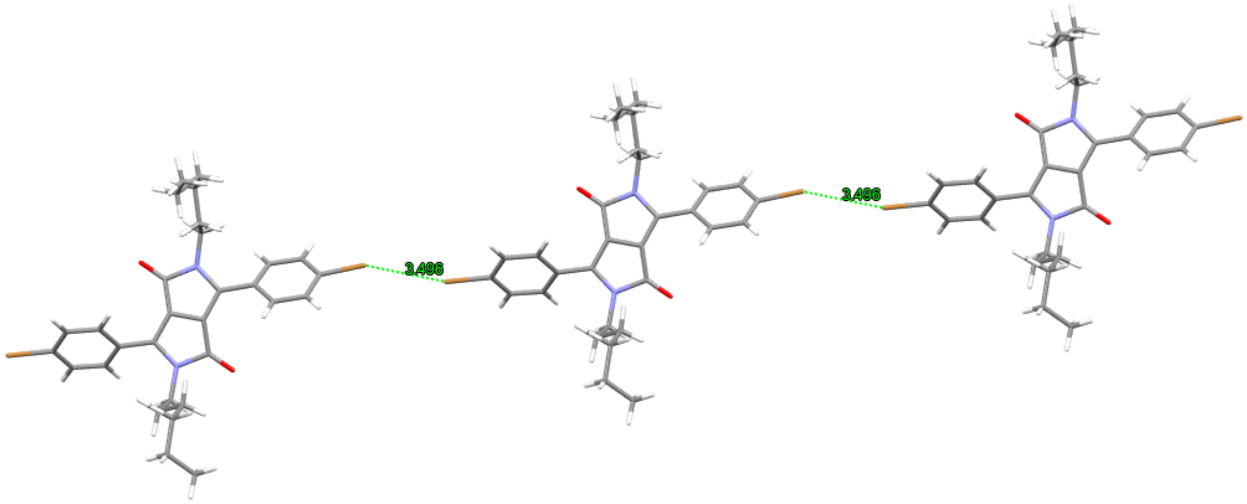

Figure S6. Crystal structure of **Br_2Hex_2DPP** showing halogen-halogen interaction.

4 – Prochirality and rotomerisation

The **Br_2Hex_2DPP** molecule is non-chiral in the gas and solution phase but is prochiral upon confinement to a surface. This surface-induced chirality, with the *M* and *P* enantiomers labelled, is shown in Figure S7.

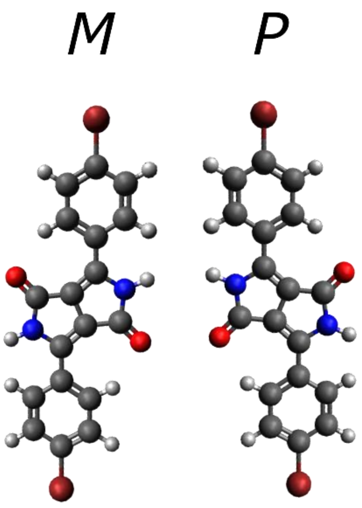

Figure S7 – *Shows the two prochiral confirmations of* ***Br_2Hex_2DPP*** *when confined to a surface (hexyl chains are omitted for clarity).*

The high degree of rotational flexibility of the C-C bond between the hexyl side chains and the DPP core leads to the possibility of different conformational isomers of **Br_2Hex_2DPP** being present on the surface. The 'arms' (hexyl side chains) can be considered in one of two orientations: position 1, where the arm is closer to the oxygen atom on the core, and position 2, where the arm points away from the oxygen (see Figure S8). This leads to four possible conformations, as shown in Figure S9. On surface, both 1-2/2-1 configurations are identical, so practically there are only three distinguishable surface-confined conformations.

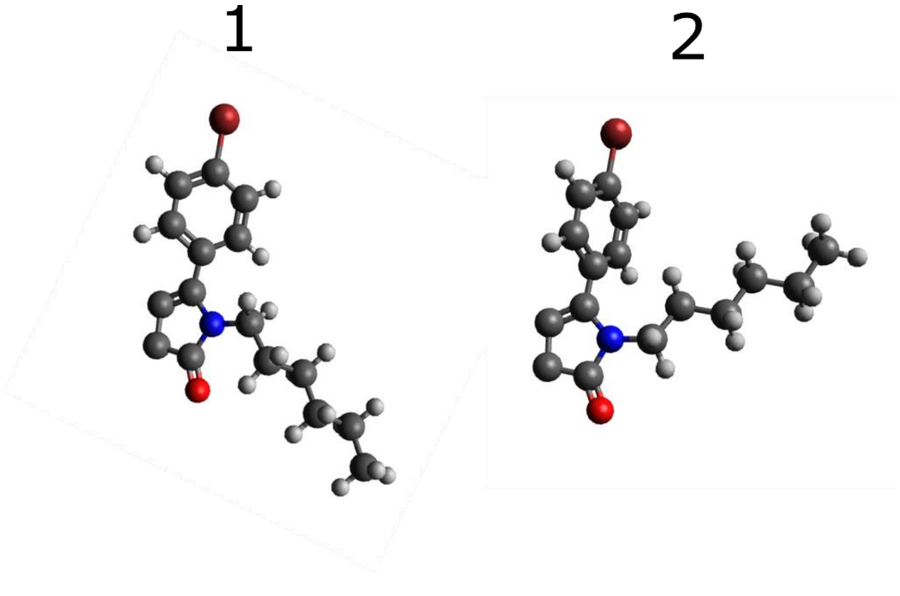

Figure S8 – *Shows the possible alkyl 'arm' positions for* ***Br_2Hex_2DPP*** *(the molecule has been truncated to focus on the alkyl chain position – the fragment shown does not represent a stable species).*

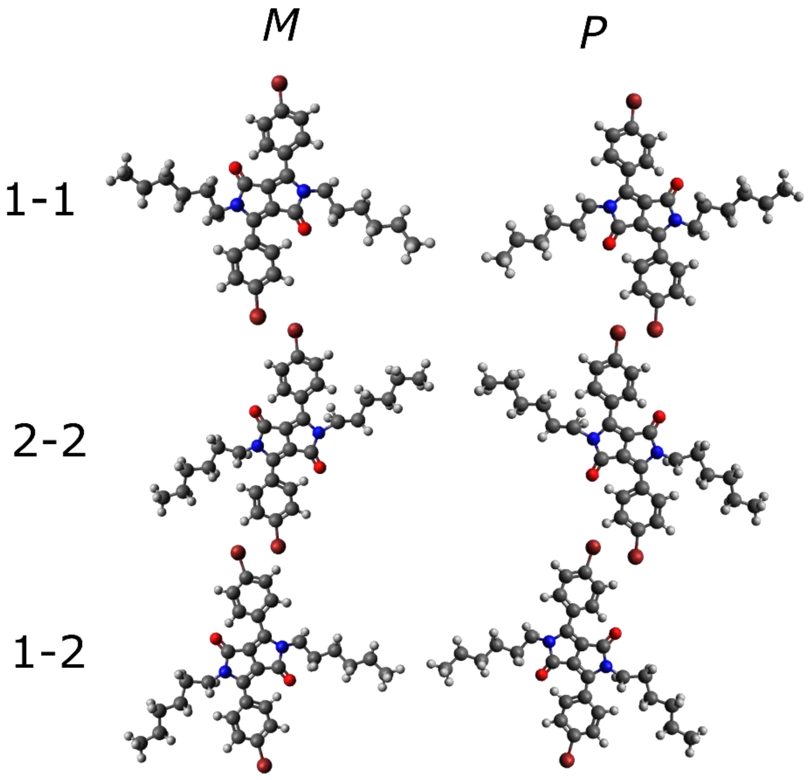

Figure S9 – *Shows all chiral rotomers for* ***Br$_2$Hex$_2$DPP*** *(1-2 and 2-1 are indistinguishable for molecules adsorbed at a surface).*

5 – Details of chirality within polymer chains

The homochiral nature, (*M*)*n* or (P)*n*, is confirmed via a comparison with the racemic, *P*-(*M*-*P*)*n*-*M*, structure (Figure S10). Alignment of the homochiral polymer structure provides good agreement with respect to the bright/high regions within the topographic STM images (assigned to the aromatic species within the polymer chains), whereas the racemic polymer structure does not spatially align with the observed linear structure of the polymer.

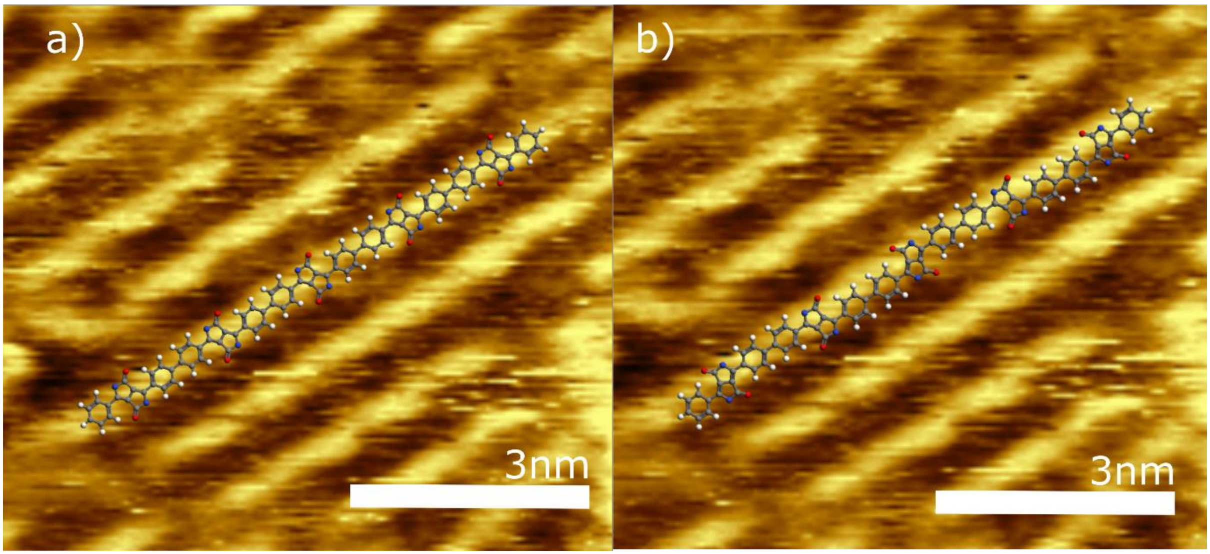

Figure S10: *STM images of the polymer structures formed following annealing of the deposited* ***Br_2Hex_2DPP*** *material to 100°C. Overlays of the proposed molecular structures for a homochiral (a) and a racemic, P-(M-P)n-M, polymer (b). The overlayed structures are positioned such that the bright contrast within the image is aligned to the aromatic regions of the polymer. Good agreement is found for homochiral structure, whereas the racemic structure does not match with the regions of bright contrast. NB hexyl chains have been removed from the molecular structure for clarity. Image parameters: Bias = 2 V, Current = 40 p.*

6 – Liquid STM

Prior to successful ultra-high vacuum (UHV) thermal deposition of **Br_2Hex_2DPP**, the molecule was successfully deposited onto both highly oriented pyrolytic graphite (HOPG) and Au(111)/Mica from solution *via* drop-casting, and imaged using an Agilent N9448A scanning tunnelling microscope (STM) under ambient temperature and pressure. **Br_2Hex_2DPP** was dissolved in toluene to give concentrations of: 2 µg/ml, 20 µg/ml, 100 µg/ml, 500 µg/ml, 1mg/ml, 2mg/ml. Subsequently, and optionally, nonanoic acid was drop-cast onto the sample to aid with imaging.

Similar to the self-assembled **Br_2Hex_2DPP**, structures seen under UHV conditions, and discussed within the main manuscript, models of possible molecular orientations were produced (Figures S11, S12 and S13): based upon STM measurements of the lattice and by assembling models based on common bonding motifs, such as hexyl chain interactions, plausible models for the molecular domains were developed. Figure S11 highlights a commonly seen structure, characterised by rows of bright features with clear horizontal and vertical periodicity (~1.5nm and 1nm respectively). This structure follows expected bonding motifs such as hexyl chain interaction, and bears similarities to those observed under UHV, however in this model there is no obvious indication of halogen bonding. Another notable feature of this structure is that the '2-2' arm conformation is preferred, and is most common across all visible structures. The close-packed structures enabled by this confirmation allow the unit-cell area to be minimised, and potentially explains their prevalence on the surface.

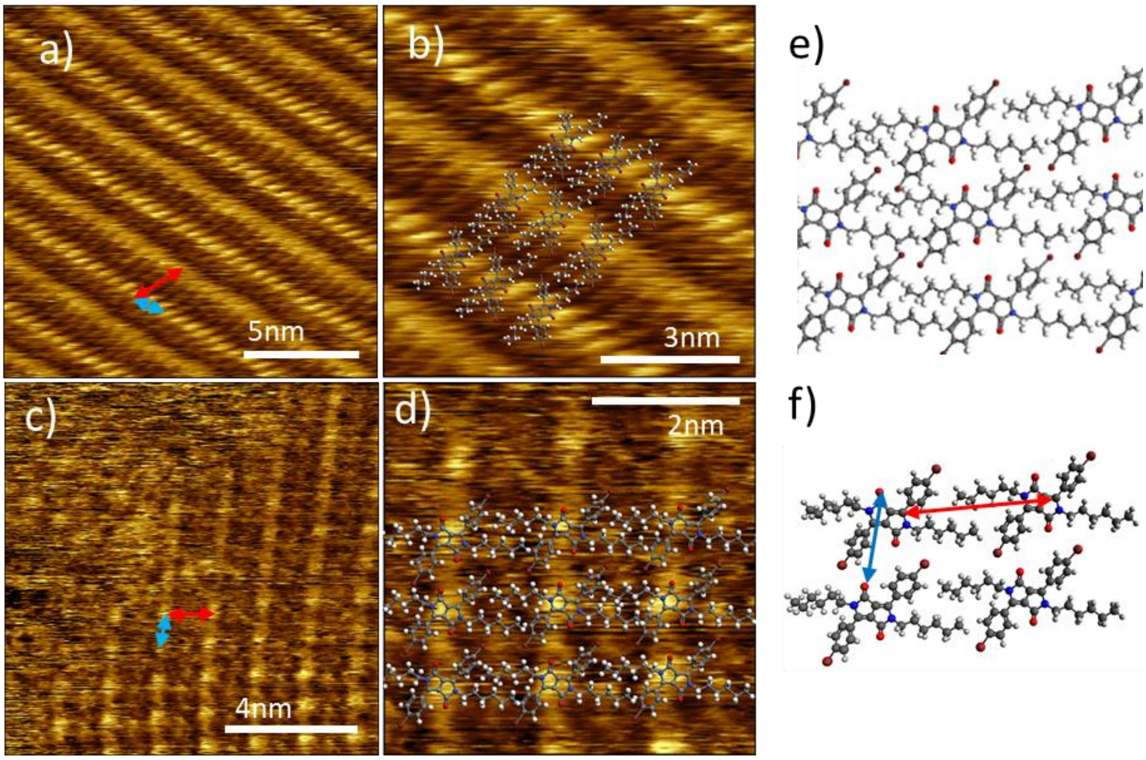

Figure S11 *- a) STM image of a lattice seen at 2mg/ml concentration drop deposited on HOPG. Horizontal spacing = 1.49 ± 0.13 nm, and the vertical spacing is 1.07 ± 0.08 nm - (Sample bias = 1 V, I(set-point) = 0.05 nA). b) Shows the proposed* ***Br_2Hex_2DPP*** *structure overlaid on the structure from (a). c) Shows a lattice seen at 500 µg/ml drop deposited on Au without nonanoic acid present. Horizontal spacing = 1.38 ± 0.09 nm, vertical spacing = 0.94 ± 0.08 nm - (Sample bias = 1 V, I(set-point) = 0.05 nA). d) Shows the proposed* ***Br_2Hex_2DPP*** *structure overlaid on the structure from (c). e) Shows the proposed structure isolated from any background image. f) Shows a single unit cell of this lattice. Horizontal spacing is measured at 1.5 nm, vertical spacing at 1 nm in this model. All overlays created using LMAPper.*[7]

An additional structure seen under ambient conditions is shown in Figure S12. This structure is of interest as it appears to incorporate the co-deposited nonanoic acid within the assembled structure. This kind of behaviour has been seen before in self assembled structures of DPP based molecules.[8]

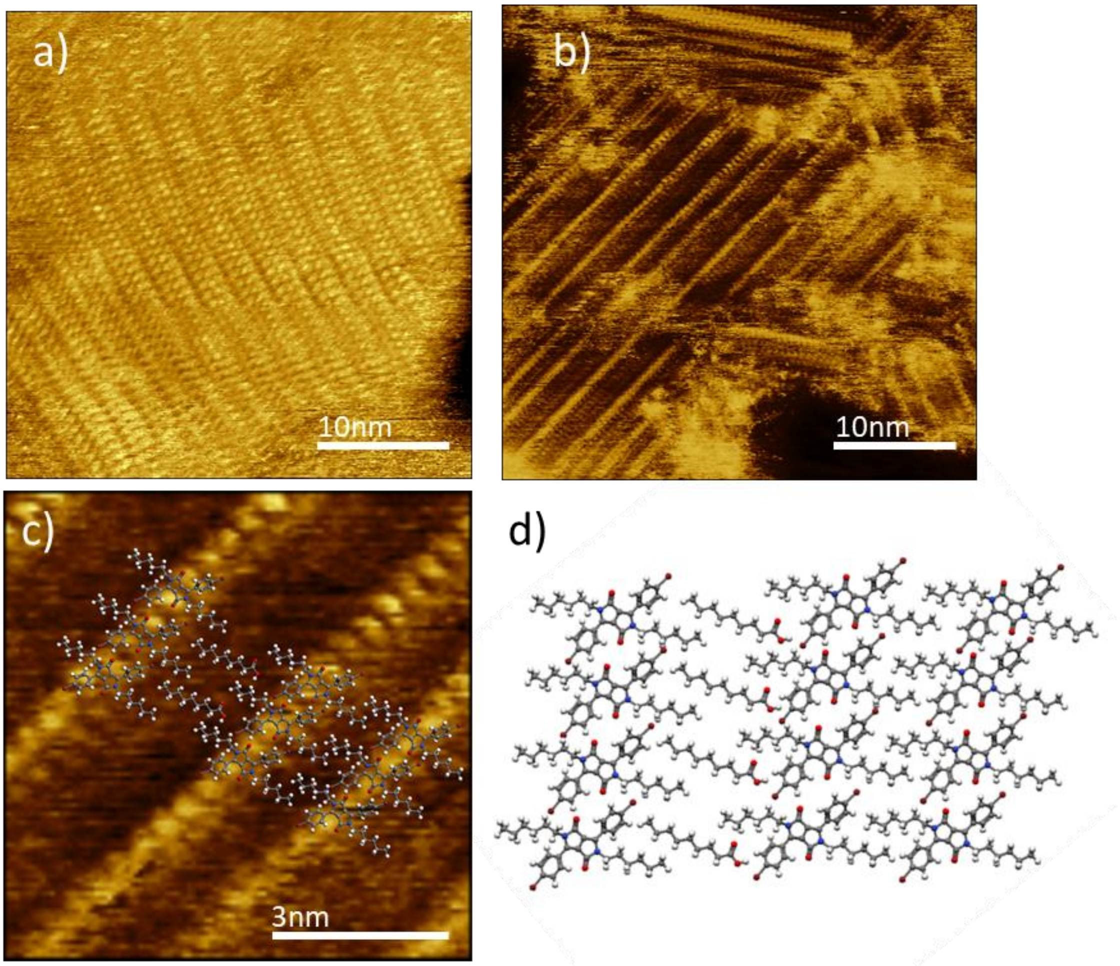

Figure S12 *- a) Shows a lattice seen at 500 µg/ml concentration drop deposited on Au, with nonanoic acid. The horizontal separation is 2.5 ± 0.1 nm. (Sample bias = 1V, I(set-point)= 0.05 nA) b) Shows a lattice seen at 1 mg/ml concentration drop deposited on Au, with nonanoic acid. The larger line spacing is 2.60 ± 0.08 nm, and the smaller line spacing is 1.75 ± 0.1 nm. (Sample bias = 1V, I(set-point) = 0.05 nA). c) Shows a proposed* ***Br_2Hex_2DPP****/nonanoic acid structure superimposed over the structure from (b). The separation between the larger spaced lines is as expected for two rows of* ***Br_2Hex_2DPP*** *separated by a single molecule of nonanoic acid, and the separation of the two closer rows is what would be expected if no nonanoic acid were involved. d) Shows the proposed* ***Br_2Hex_2DPP****/nonanoic acid structure.*

Many other structures were seen at the various concentrations, and on different surfaces, including an unusual hexagonal structure, shown in Figure S13. While stable structures were obtained *via* liquid deposition, attempts at thermally initiated polymerisation were unsuccessful. Methodologies involving heating to 250°C within an inert gas (nitrogen) tube furnace, under vacuum, and under ambient pressure and gas mixtures were attempted.

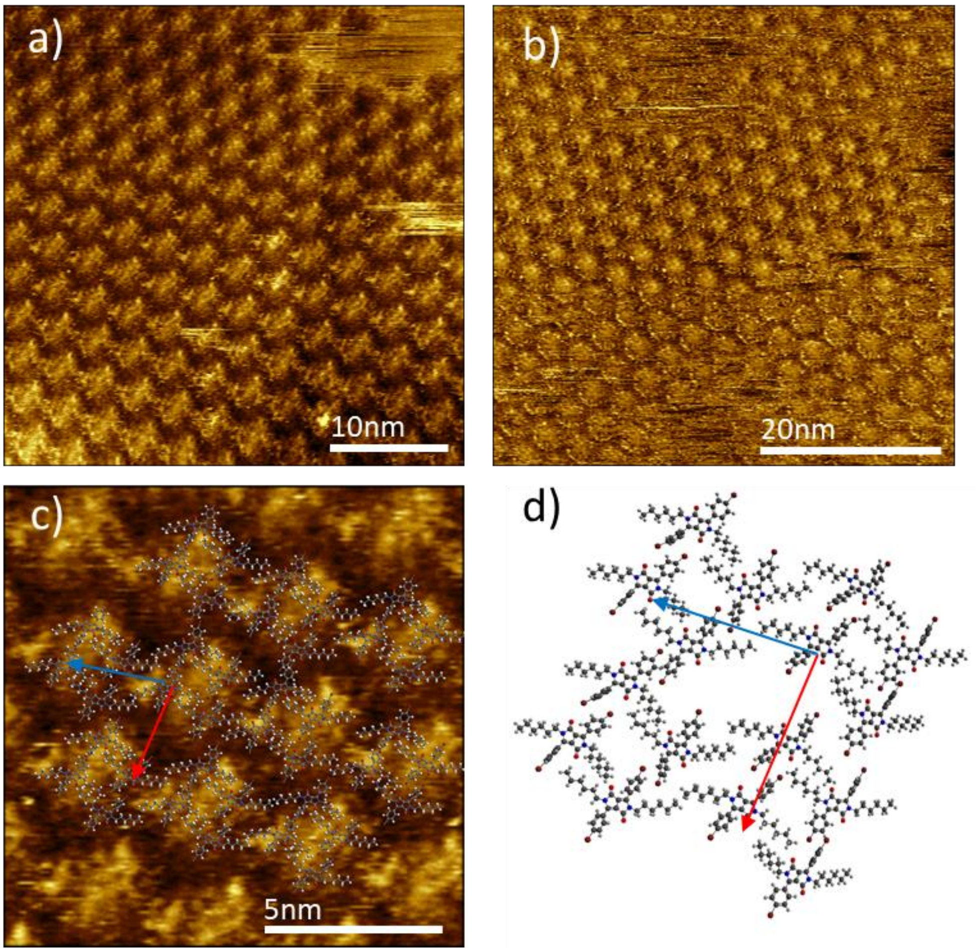

Figure S13 - *a-b) STM images showing structures seen at 500 µg/ml drop deposited on HOPG. (Sample bias = 1 V, I(set-point) = 0.05 nA) c) Shows the structure from (a) with overlaid proposed* ***Br_2Hex_2DPP*** *structure and lattice vectors. The blue arrow representing the horizontal vector was measured to be 3.3 ± 0.2 nm, and the vertical vector was measured to be 2.9 ± 0.1 nm. d) Shows a model of the molecular structure, where the blue length was measured to be 3.1 nm and the red length was measured to be 2.9 nm.*

7 – Example line profiles of polymers formed from Br$_2$Hex$_2$DPP following annealing at 100^{o}C

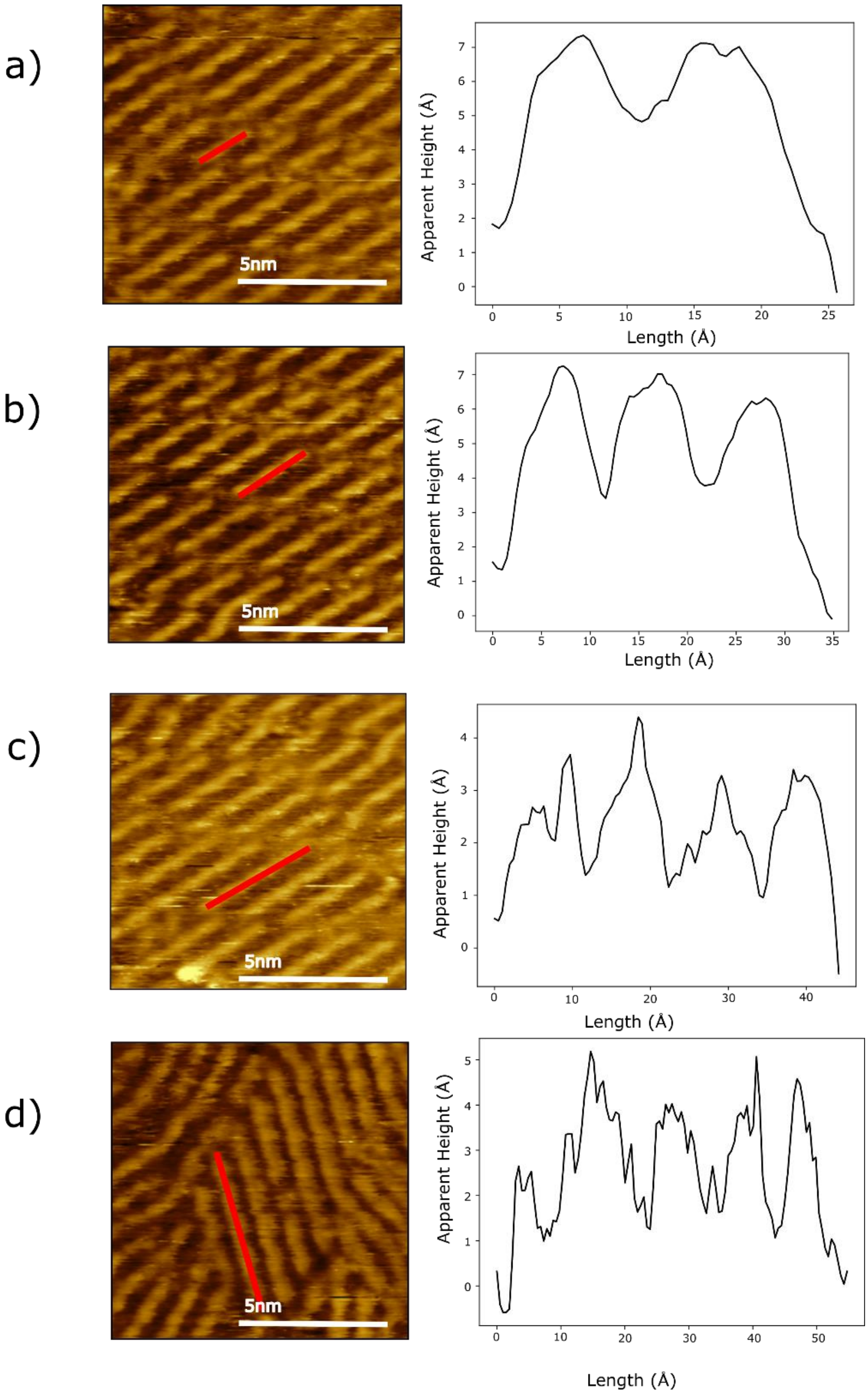

Figure S14 – *STM images and associated line profiles taken along DPP-based polymer chains of different lengths following annealing at 100^{o}C (location of line profile indicated on the STM image by a red line). a) Polymer chain measured to be approximately 1.2 nm in length, likely to be a single debrominated* ***Br$_2$Hex$_2$DPP*** *species. b) Chain measured to be approximately 2.2 nm in length and is suggested to be a debrominated* ***Br$_2$Hex$_2$DPP*** *dimer. c) Chain is measured to be approximately 3.3 nm in length and is suggested to be a debrominated* ***Br$_2$Hex$_2$DPP*** *trimer. d) Chain is measured to be approximately 4.3 nm in length and is suggested to be a debrominated* ***Br$_2$Hex$_2$DPP*** *tetramer. Images taken with Sample bias = 2 V, I(set-point) = 40 pA.*

8 – XPS Results

X-ray photoelectron spectroscopy (XPS) data was acquired for **Br_2Hex_2DPP** on Au(111). Figure S15 shows the C1s region both before and after annealing to 350°C. The peaks have the same form and a similar binding energy. Figure S16 shows the O1s region, with no identifiable peaks.

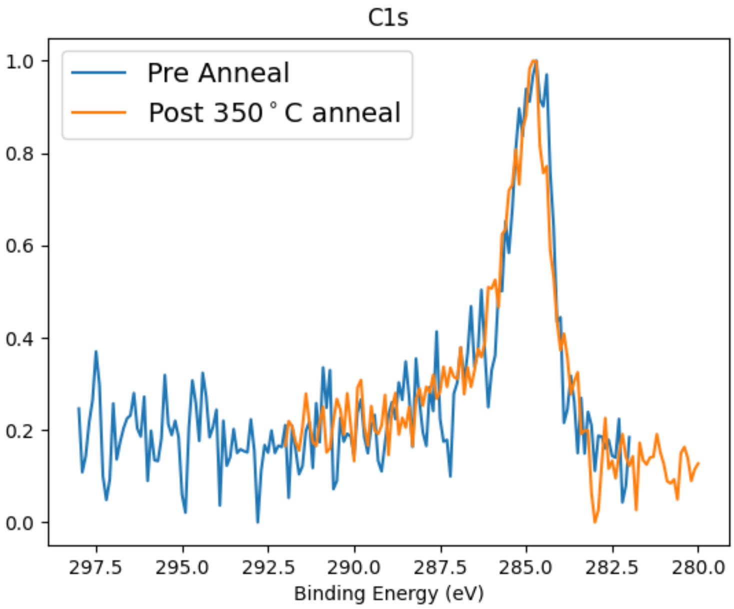

Figure S15 - *C1s XPS region for* **Br_2Hex_2DPP** on Au(111)*, before and after annealing to 350°C. The spectra have been backgrounded on the low binding energy extreme and normalised to the highest point in the spectra for comparison of the lineshapes.*

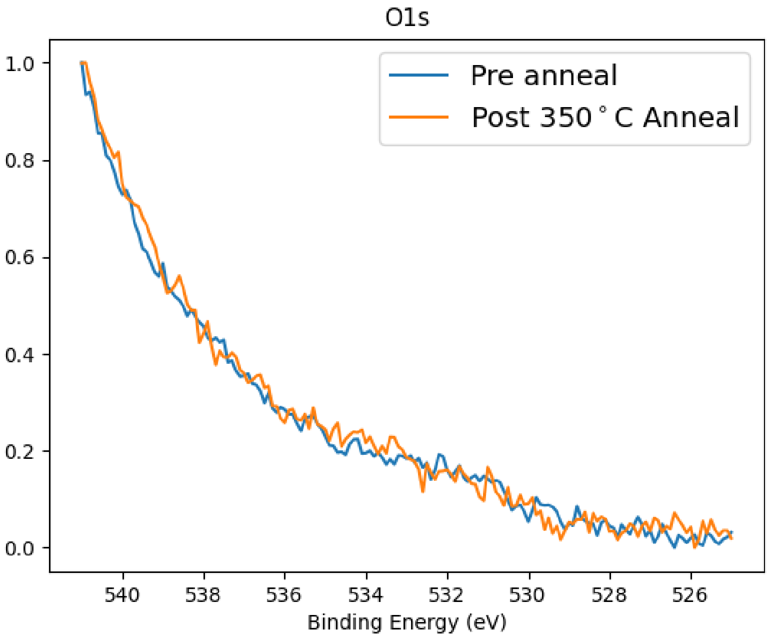

Figure S16 - *O1s XPS region for* **Br_2Hex_2DPP** on Au(111)*, before and after annealing to 350°C. The spectra have been backgrounded on the low binding energy extreme and normalised to the highest point in the spectra for comparison of the lineshapes.*

9 – Chain separation measurements

Polymer chain separation was measured by identifying approximately parallel chains and acquiring a line profile perpendicular to the length of the chain, as shown in figure S17. From these line profiles, peak-to-peak measurements were used to determine line separation. Measurements were performed for both forwards and backward scans, with an average of the two measurements taken, to minimise the effect of drift.

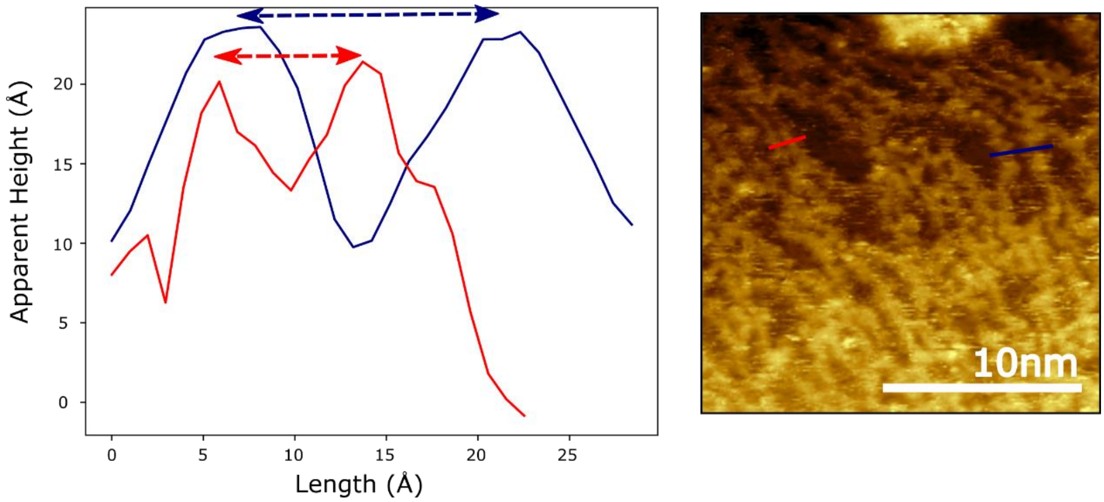

Figure S17 – *Two line profiles demonstrating the separation between polymers (profile locations are indicated within the STM image). The peak-to-peak separation on the red and blue line profiles are 8 Å and 14 Å, respectively. The STM image shows a* ***Br_2Hex_2DPP****/Au(111) surface following annealing at 200°C (Sample bias = 2 V, I(set-point) = 200 pA).*

10 – Molecular Modelling

Molecular models of the observed self-assembled structures were determined by the steps as shown in figure S18: (a) measuring molecular lattices acquired from STM via an autocorrelation function, (b) matching the expected dimensions of **Br_2Hex_2DPP** to features within a 2DFFT filtered image of the lattice using LMAPper[1], (c) modelling these lattices within Avogadro matching the dimensions of the lattice, typically in a 9x9 grid, (d) using simple molecular mechanics (MMFF94) to allow the molecules to flex, and constructing a unit cell using the central molecule from the 9x9 grid matching the measured lattice dimensions, (e) creating an idealised model based on this unit cell, featuring the rotated rings and flatter arm chains, and (f) overlaying this unit cell onto the 2DFFT. Using this method, we were able to determine that the unit cell shown in S18e) was the most plausible, as the solution presented by simple molecular mechanics showed a limited deviation from planarity, minimised steric interactions, and featured several common self-assembly motifs (alkyl chain interdigitation, halogen bonding, and π – π interactions of aryl rings). Our proposed model has an oxygen-bromine separation of ~2.5-2.8 Å. This is smaller than the Br-Br halogen bond we observe in our crystallography data (~3.5 Å – See Figure S6) but is not dissimilar to previously reported O-X type halogen bonding.[9] This homochiral domain may exist in either the *M* or *P* chirality (based upon molecular overlays upon STM images), although identification of individual molecular chiralities is not possible at this resolution.

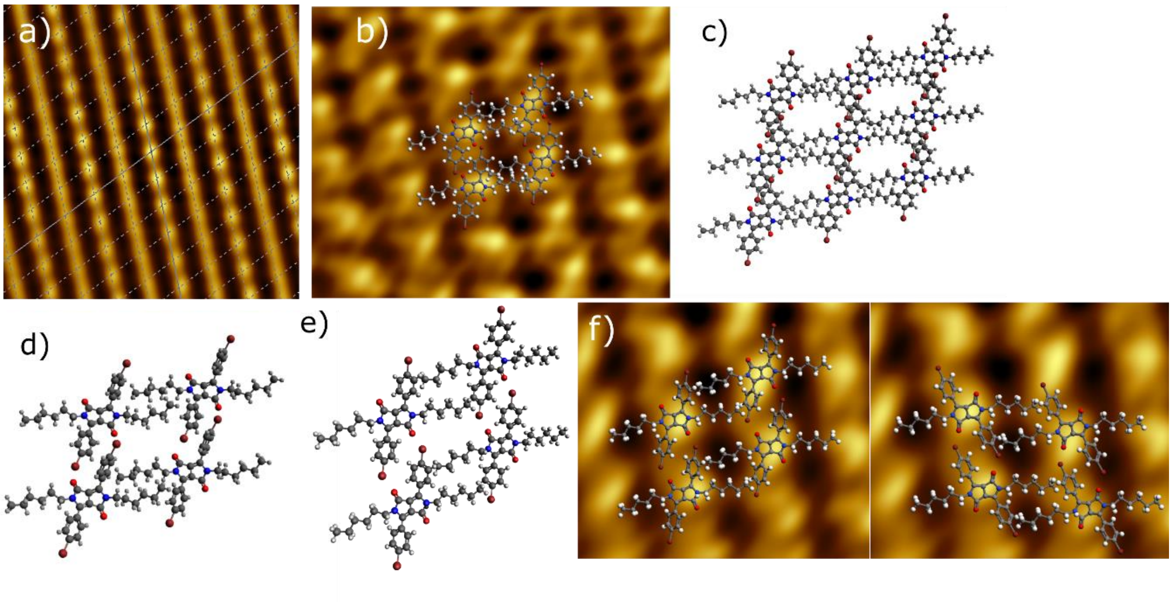

Figure S18 *– a) Measuring the lattice dimensions of the self-assembled lattice via use of an autocorrelation function. b) Overlaid simple* ***Br_2Hex_2DPP*** *homochiral molecular model onto a masked 2DFFT of the lattice. c) The molecular model from b) recreated in Avogadro, with lattice dimensions matching those measured. d) A model unit cell created using the central molecule from the 9x9 grid shown in c), after the application of molecular mechanics calculations, placed at the dimensions measured from the lattice. e) An idealised unit cell created using the motifs of this calculated unit cell, featuring the rotated rings. f) This unit cell overlaid onto the 2DFFT filtered image. Both chiralities (M and P) within a homochiral domain fit with the acquired STM data. (Bias = 2 V, Current =20 pA)*

Other models were considered, as shown in figure S19. These models were considered less plausible, as a reasonable degree of planarity was not possible to achieve, as significant sections of the molecule were observed to overlap. On this basis we are able to discount heterochiral domains, and domains where molecular orientation is roated.

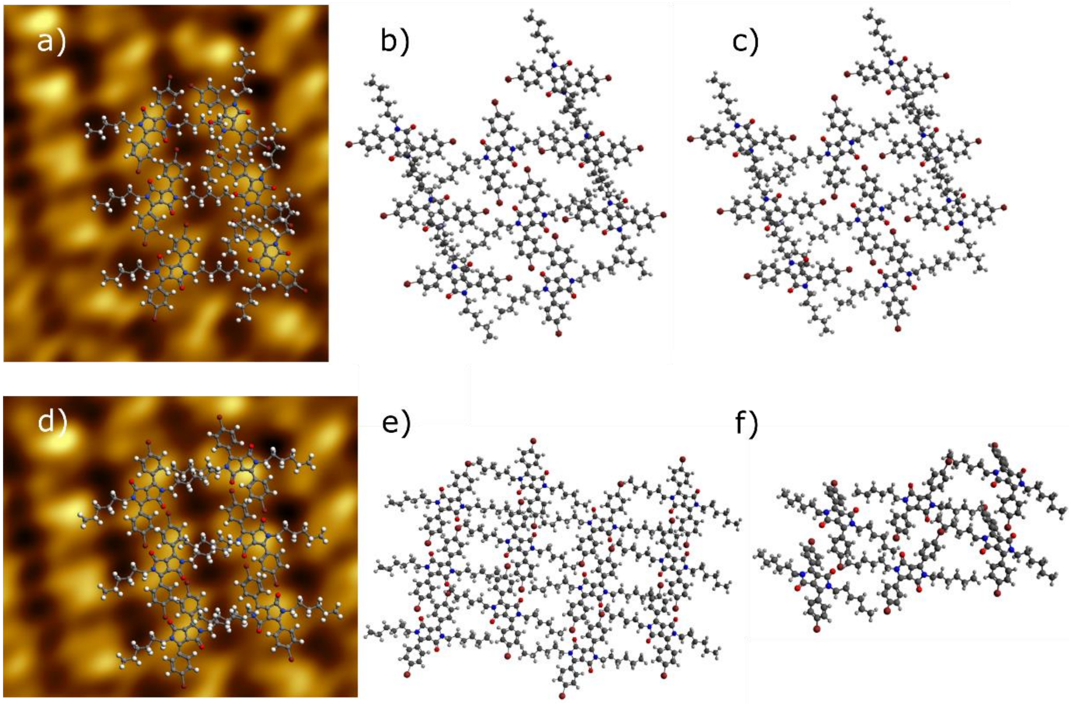

Figure S19 – *a) Overlaid simple* ***Br$_2$Hex$_2$DPP*** *homochiral alternating rotation model onto a 2DFFT filtered image of the molecular lattice. b) The molecular model from a) recreated in Avogadro, with lattice dimensions matching those measured experimentally. c) The molecular model from b) once simple molecular mechanics have been applied; many segments still overlap, in contrast to what would be expected for a surface confined system. d) Overlaid simple* ***Br$_2$Hex$_2$DPP*** *racemic alternating chirality model onto a 2DFFT filtered image of the molecular lattice. e) The molecular model from d) recreated in Avogadro, with lattice dimensions matching those measured, in 4x3 grid, to create a central molecule for both chiralities. f) The resultant unit cell for a racemic alternating chirality lattice. As can be seen, there are still a great number of possible steric clashes in a proposed "flat" model of this lattice.*

11 – Tip changes during STM

STM images acquired under UHV conditions at ambient temperature, frequently displayed tip instability. Figure S20, demonstrates typical contrast changes.

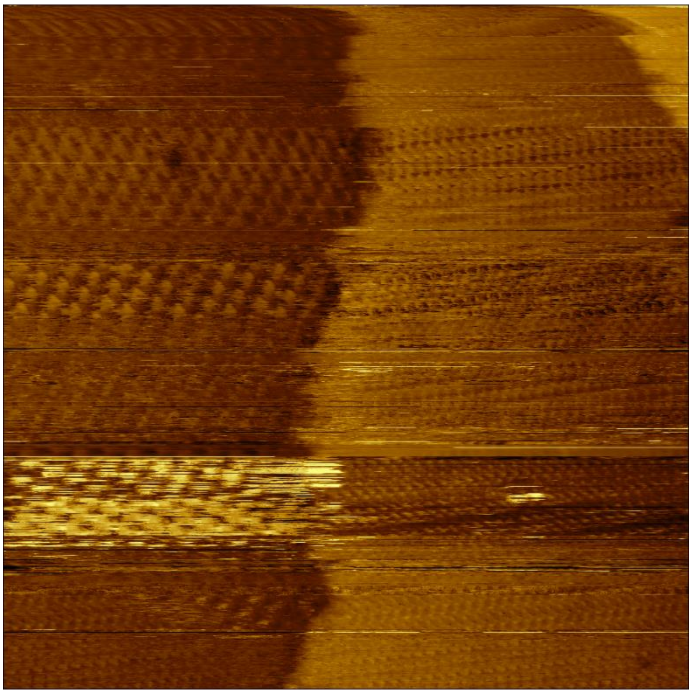

Figure S20 – *Shows regular tip changes during imaging of the* **Br_2Hex_2DPP** *on Au(111) (Sample bias = 2 V, I(set-point) = 25 pA).*

12 – Details on crosslinking and image resolution

The change in image quality following anneal temperatures above 100 °C may be attributed to the cleaving of the hexyl chains, which is likely to lead to an increase in the amount diffusing material present on the surface, which in turn will affect tip stability and ultimately image quality. Another factor is that as the hexyl chains remaining intact at 100 °C, the interdigitation of these chains stabilises the surface structure significantly, allowing for more stable imaging. At higher temperatures the loss of chains results in a corresponding reduction in stability of molecular structures. The possibility of cross linking at the lower temperatures cannot be wholly dismissed, however the features we ascribe to crosslinking behaviour are more frequently observed upon annealing to 350 °C; these features are highlighted in Figure S21.

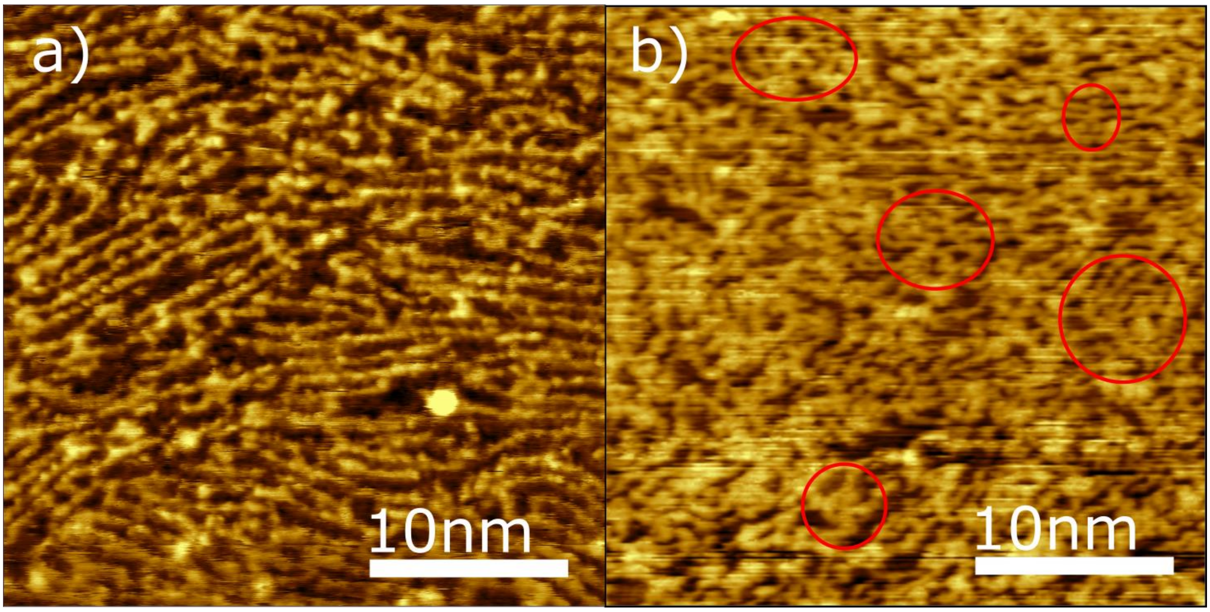

Figure S21 – *a) An STM image (Bias = 2 V, Current = 40 pA) showing polymer chains as seen after annealing to 200°C. b) An STM image (Bias = 2 V, Current = 20 pA) showing polymer chains after annealing to 350°C, with instances of crosslinking highlighted with red circles.*

13 – Chain angle plots for chains at 100^{o}C and 250^{o}C

The angles of chains relative to the scan direction were taken for several images of chains after annealing to 100 ^{o}C and 200-250 ^{o}C. The angular orientations of these chains are shown in Figure S22.

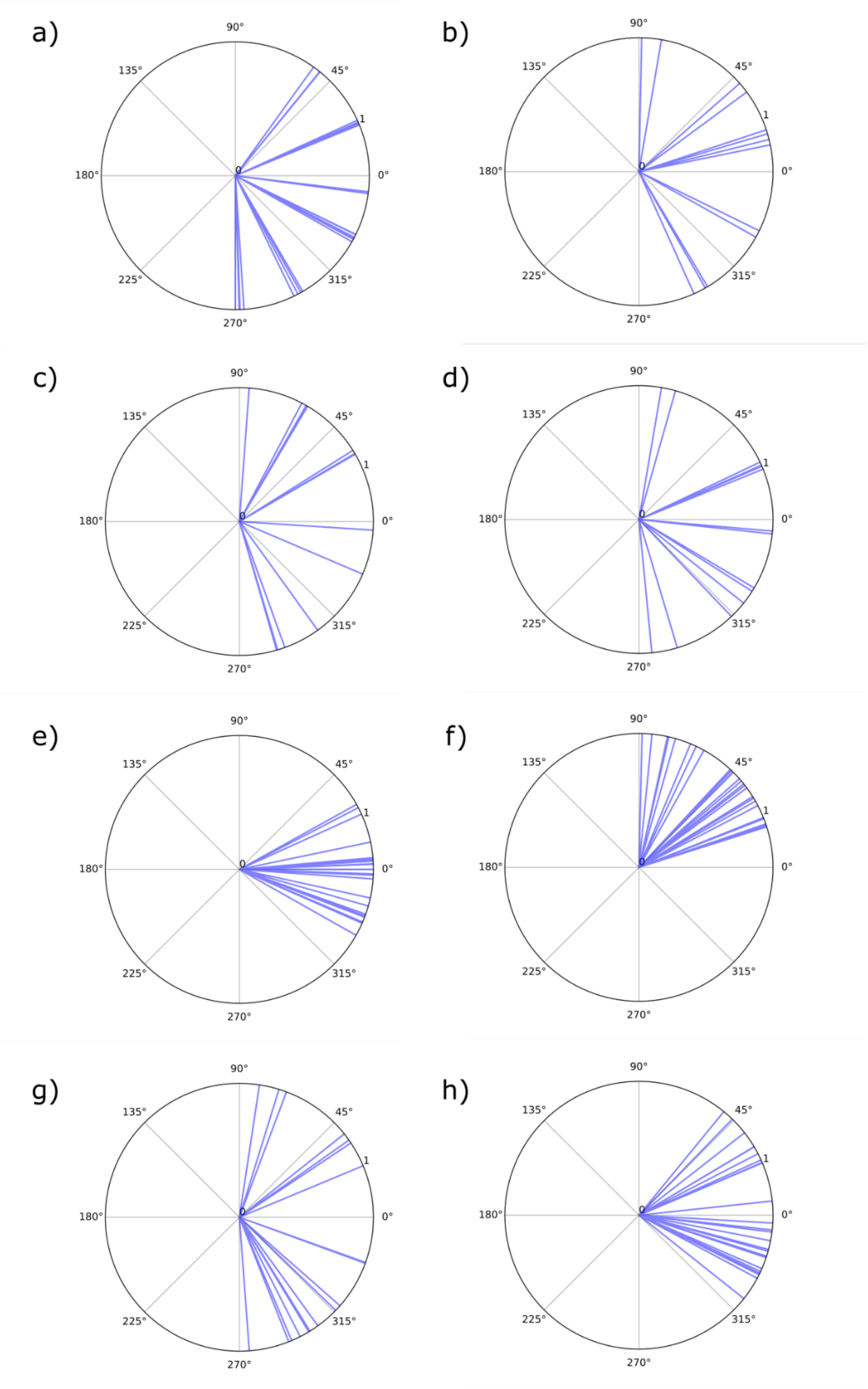

Figure S22 – *(a-d) Show orientations of chains seen after 100^{o}C anneal. (e-g) Show orientations of chains seen after 200-250^{o}C anneal.*

14 - Bibliography

1 J. Cosier, A.M. Glazer, *J Appl Crystallogr*, 1986, **19**, 105-107.

2 Rigaku Oxford Diffraction, *CrysAlisPro Software system, version 1.171.40.45a*, Rigaku Corporation, Oxford, UK. n.d (2018).

3 O.V. Dolomanov, L.J. Bourhis, R.J. Gildea, J.A.K. Howard, H. Puschmann, *J Appl Crystallogr*, 2009, **42**, 339-341.

4 G.M. Sheldrick, *Acta Crystallogr A*, 2015, **71**, 3-8.

5 G.M. Sheldrick, *Acta Crystallogr Sect C Struct Chem*, 2015, **71**, 3-8.

6 **CheckCIF** http://checkcif.iucr.org.nottingham.idm.oclc.org

7 L. Perdigao, *Date Accessed 7.5.21*, 2019, **LMAPper**, www.Aceforge.net/projects/spm-and-mol-viewer.

8 C. Fu, P. J. Beldon and D. F. Perepichka, *Chem. Mater.*, 2017, **29**, 2979–2987.

9 G. Cavallo, P. Metrangolo, R. Milani, T. Pilati, A. Priimagi, G. Resnati, and G. Terraneo *Chem. Rev.* 2016, **116**, 4, 2478–2601.